Self-healing of a pre-notched WS2/a-C coating

Cao, Huatang; De Hosson, J.T.M.; Pei, Yutao T.

Published in:
Materials Research Letters

DOI:
10.1080/21663831.2018.1561538

Publication date:
2018

Materials Research Letters

ISSN: (Print) 2166-3831 (Online) Journal homepage: http://www.tandfonline.com/loi/tmrl20

Self-healing of a pre-notched WS_2/a-C coating

Huatang Cao, Jeff Th.M. De Hosson & Yutao Pei

To cite this article: Huatang Cao, Jeff Th.M. De Hosson & Yutao Pei (2019) Self-healing of a pre-notched WS_2/a-C coating, Materials Research Letters, 7:3, 103-109, DOI: 10.1080/21663831.2018.1561538

To link to this article: https://doi.org/10.1080/21663831.2018.1561538

Published online: 24 Dec 2018.

MATER. RES. LETT.
2019, VOL. 7, NO. 3, 103–109
https://doi.org/10.1080/21663831.2018.1561538

MATERIALS RESEARCH LETTERS
Taylor & Francis
Taylor & Francis Group

ORIGINAL REPORTS

Self-healing of a pre-notched WS_2/a-C coating

Huatang Cao[a], Jeff Th.M. De Hosson[b] and Yutao Pei [a]

[a]Department of Advanced Production Engineering, Engineering and Technology Institute Groningen, Faculty of Science and Engineering, University of Groningen, Groningen, the Netherlands; [b]Department of Applied Physics, Zernike Institute for Advanced Materials, Faculty of Science and Engineering, University of Groningen, Groningen, the Netherlands

ABSTRACT

This letter reports that a pre-notched WS_2/a-C tribocoating surface can be fully healed through sliding. The healed notches act as superior lubricant micro-reservoirs affording frictionless responses leading to an ultralow coefficient of friction (0.02). HR-TEM observations reveal WS_2 (002) platelets in the healed notch parallel to the outer coating surface and to the V-notch/coating interface. Direct evidence of the rearrangement of WS_2 at the curved interface elucidates that basal plane reorientation does not occur necessarily parallel to the counterpart sliding direction as was taken for granted in literature. The patchy tribofilm provides a new avenue for self-healing efficiency in tribology.

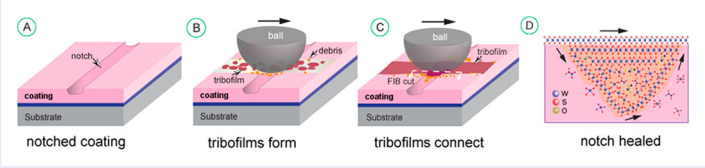

IMPACT STATEMENT

This research reveals a new avenue for self-healing and repairing of damage in tribocoatings whereby one may lift the requirement of producing defect-free coatings for triboapplications.

ARTICLE HISTORY
Received 6 November 2018

KEYWORDS
Self-healing; WS_2; basal plane reorientation; tribocoating; HR-TEM

1. Introduction

Engineering materials accumulate damages during their use in service. Component failure or functional losses may consequently take place once damage exceeds a critical value. Failure readily occurs under extreme conditions, e.g. fatigue and environmental attacks. If a material system could self-heal or reverse the damage accumulation, the sustainability will be substantially enhanced, together with considerable savings of resources and energy [1]. Self-healing materials have the ability to repair themselves autonomously and thus recover functionality [2]. In practice, however, self-healing phenomenon is not fully autonomous but is stimulated either by the occurrence of damage itself or by external stimuli such as load and heat [1]. Various explorations have been reported including microencapsulated liquid agents [3], polymer crosslinking [2], shape memory alloy wires [4], microbial healing [5,6], and high-temperature ceramic oxidations [7,8]. However in the field of lubricating tribocoatings where the anti-wear takes priority as the prime concern, very scant information has been reported on their self-healing capabilities.

In tribological applications, intrinsic cracks may propagate along columnar boundaries, branch and could even trigger catastrophic spalling of the coating. Various advancing approaches such as applying an interlayer [9], controlling the target-substrate distance [10], tuning the microstructure [11,12] and doping with carbon or metallic elements [13,14] were employed to enhance the mechanical response of the coating under different extreme conditions. It turned out rather difficult to produce defect free coatings.

Among appealing lubricants, transition-metal dichalcogenides (TMD) such as WS_2 excel due to their unique anisotropic crystal structure, namely hexagonal units where layers of W atoms are sandwiched in-between layers of packed sulfur atoms. The bonding within each unit, i.e. the M-X bond is covalent, while

CONTACT Yutao Pei y.pei@rug.nl Department of Advanced Production Engineering, Engineering and Technology Institute Groningen, Faculty of Science and Engineering, University of Groningen, Nijenborgh 4, Groningen, 9747AG, the Netherlands

Supplemental data for this article can be accessed here. https://doi.org/10.1080/21663831.2018.1561538

the different units are maintained through weak Van der Waals interactions. Slip occurs preferentially between the (002) lamellae of low shear strength ($\tau = 1$–2 MPa) yielding ultralow friction [15]. However, WS_2 coatings made with a sputtering technique are often columnar-like, porous with microcracks [16,17]. Fortunately, the tribofilm formed during wear may act as a self-lubricating layer isolating metal-to-metal contact leading to a reduction of friction in ambient conditions. HR-TEM observations in-situ under the wear track reveal subsurface reorientations of TMD platelets, where their basal planes are realigned parallel to the coating surface into the 'frictionless' (002) direction [9,10]. This stimulated us to explore the following idea: by sliding contact, segmented TMD nanoplatelets are reorientated and bridged to form a closed continuous tribofilm that may consequently repair damages in an adaptive way.

2. Experimental

A nanocomposite WS_2/a-C coating was deposited on a single crystal silicon(100) wafer with a TEER UDP400/4 closed-field unbalanced magnetron sputtering system. The substrate was ultrasonically cleansed in acetone before Ar plasma etching for 20 min at −400 V bias voltage (p-DC mode). Two WS_2 targets powered at 0.5A (150 kHz, 62.5% duty cycle) were co-sputtered with one graphite target (0.5A, DC mode). The substrate was mounted vertically on a carousel holder that rotated at 3 rpm in front of the targets. A Cr interlayer ($\sim$ 300 nm thick) was deposited to facilitate the interfacial adhesion between the coating and substrate. First we used a CSM scratch tester to deliberately induce a notch (2–5 μm wide) on the surface of the coating, which supposes to mimic damages caused in real service. Thereafter tribotests ran for 10,000 laps using a CSM ball-on-disk tribometer against a ø6 mm 100Cr6 ball at a sliding speed of 10 cm s^{-1} (wear track diameter 15 mm, relative humidity 5–7%). The counterpart ball slides perpendicularly across the pre-notches. A confocal microscope was used to plot the morphology of the notch before and after sliding. Further, the microstructure was scrutinized using light microscope, Raman spectroscopy (632.8 nm Thorlabs HeNe laser, 1 mW), scanning electron microscope (ESEM, Philips FEG-XL30) and high resolution transmission electron microscope (HR-TEM, 2010F-JEOL, 200 kV). Focused ion beam (FIB, Lyra Tescan) was employed to slice the healed parts for cross sectional observation and to prepare TEM lamella over the healed notches for HR-TEM examination. Before FIB milling, a protective Pt layer was deposited for minimizing Ga ion irradiation damage.

3. Results and discussion

Figure 1(a,b) show the images taken with light microscopy of a wear track with the pre-notch healed after sliding in dry air. It can be seen that a smooth whitish band covers the notch in the wear track, in contrast to the untouched dark pre-notch remained on the two sides of the wear track. This is confirmed in Figure 1(b) at a higher magnification (also Figure S1(a)), where a clear tortuous band indicates that some material is filled in the notch and result in a smooth surface. To unravel the particular phases present, Raman spectroscopy was executed on selected areas 1–5 as marked in Figure 1(a,b). As shown in Figure 1(c), the raw coating of area 1 (outside of the wear track) indicates the presence of both E^1_{2g} (355 cm^{-1}) and A^1_g (421 cm^{-1}) peaks of WS_2 and typical D ($\sim$ 1380 cm^{-1}) and G ($\sim$ 1560 cm^{-1}) peaks of the amorphous carbon matrix [16], in accordance with the area 2 on the wear track. Raman spectra of area 3 and 4 reconfirm similar spectra of both the WS_2 and a-C, but with intensified signals as compared with that of area 1 and 2. It can be concluded that the transferred material in the notch (area 4) is the same as that in the wear track (area 3). In addition, active WO_3 peaks at around 800 cm^{-1} are detected in the wear debris accumulated beside the wear track (area 5 and 6). This implies that oxidation of partial WS_2 to WO_3 occurred during sliding.

Figure 1(d) shows that the coefficient of friction (CoF) is ultralow (average 0.027 within 10,000 laps) and yet very stable. Moreover, the inset in Figure 1(d) reveals that the running-in period is extremely short and the CoF drops from the peak of 0.035 to 0.02 in only 20 laps. The short running-in period corresponds to the rapid formation of lubricative tribofilm on the wear track and transfer layer on the counterbody. Previous study unveiled that sliding contact could immediately reorient WS_2 platelets at the wear interface parallel to the sliding direction, resulting in self-adaptive 'frictionless' responses [18].

Figure 2(a,b) compare SEM images of the pre-notch before and after healing. Figure 2(a) shows the notch with a variable width 2–5 μm, whereas Figure 2(b) and Figure S1(a) clearly indicate that the notch is filled and flattened. In fact, a thin cap is formed bridging the notch. Figure 2(c) compares the transverse profiles of the notch and the healed notch, where the maximum depth of the pre-notch is 0.34 μm. After healing, the notch is filled up with a slight protrusion $\sim$ 0.1 μm high. At higher magnification, SEM observations of the interface (Figure 2(d)), together with two FIB cuts (Figure 2(e,f)) that are made from the side edge towards the center of the wear track, unveil a gradual healing process. The cross-section near the edge of the wear track as displayed in Figure 2(e) shows a couple of cracks formed by scratching that

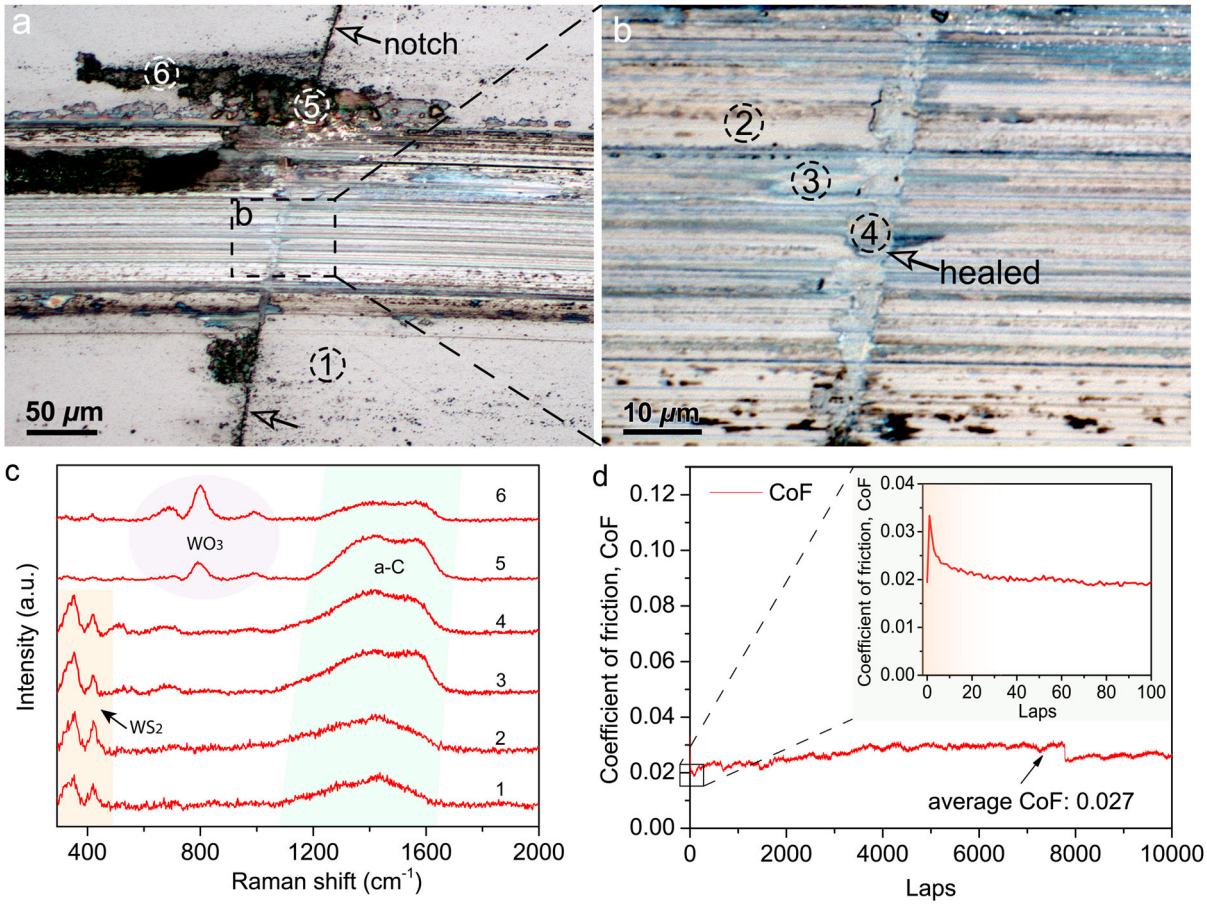

Figure 1. (a,b) images with light microscopy of a wear track on the notched WS_2/a-C coating after sliding; (c) Raman spectra of different areas as indicated in (a,b); (d) stable ultralow coefficient of friction with the inset showing a short run-in period, indicating no influence of the pre-notches on the triboperformance.

penetrate throughout the entire coating until the Cr interlayer (red arrow). Yet the cracks are still only partially recovered as indicated by the crevasse (blue arrow). Moving 10 μm towards the center of the wear track, the second FIB cut (Figure 2(f)) confirms that the notch is entirely healed without any remaining crevasses. EDS mapping of Figure S2 shows the distribution of chemical elements in the partially healed notch. In particular it is found that the distribution of W is uniform and nearly indistinguishable between regions inside and outside the healed notch. This indicates that the pre-notch has been successfully patched due to the transport of tribofilms towards the damage area. In contrast to the pre-notch made perpendicular to the wear track, scratches may often be formed in wear tracks parallel to the sliding direction due to abrasion or ploughing, as those observed near the edge of the wear track shown in Figure S1(c). From Figure S1(a,b), one could see that substantial continuous tribofilms formed on the wear track. These tribofilms effectively covered and flattened the scratches; for instance, deep scratches near the edge of the wear track were gradually being filled up/healed (see Figure S1(b,c)). It should be pointed out that, under dry sliding, wear scratches are dynamically formed and may be successively healed provided that substantial and continuous tribofilms are formed on a coating during sliding.

To further reveal the healing quality, a cross-section TEM specimen was sliced at the center part of the wear track by FIB. It clearly shows a compact and healed area underneath the Pt protecting layer (Figure 3(a)). The selected area electron diffraction (SAED) patterns (see Figure S3) conducted at the circled area 1–4 in the inset of Figure 3(a) confirm weak WS_2 (002) rings from area 2. In area 3 at the center of the healed part, WS_2 (002) and (110) planes are intensified together with a diffraction halo reflecting the stacking planes 10Z (Z = 0, 1, 2 . . .) of WS_2 [16]. In comparison with the SAED of area 4 from the raw coating, the additional WO_3 (002) plane reconfirms the oxidation of WS_2 due to the passivation of dangling bonds and active sites of edge-orientated WS_2 during sliding.

HR-TEM images of Figure 3(b–i) display a panorama view on the healed section. Figure 3(b) shows the inlet where the tribofilm flows into the notch. Arresting WS_2

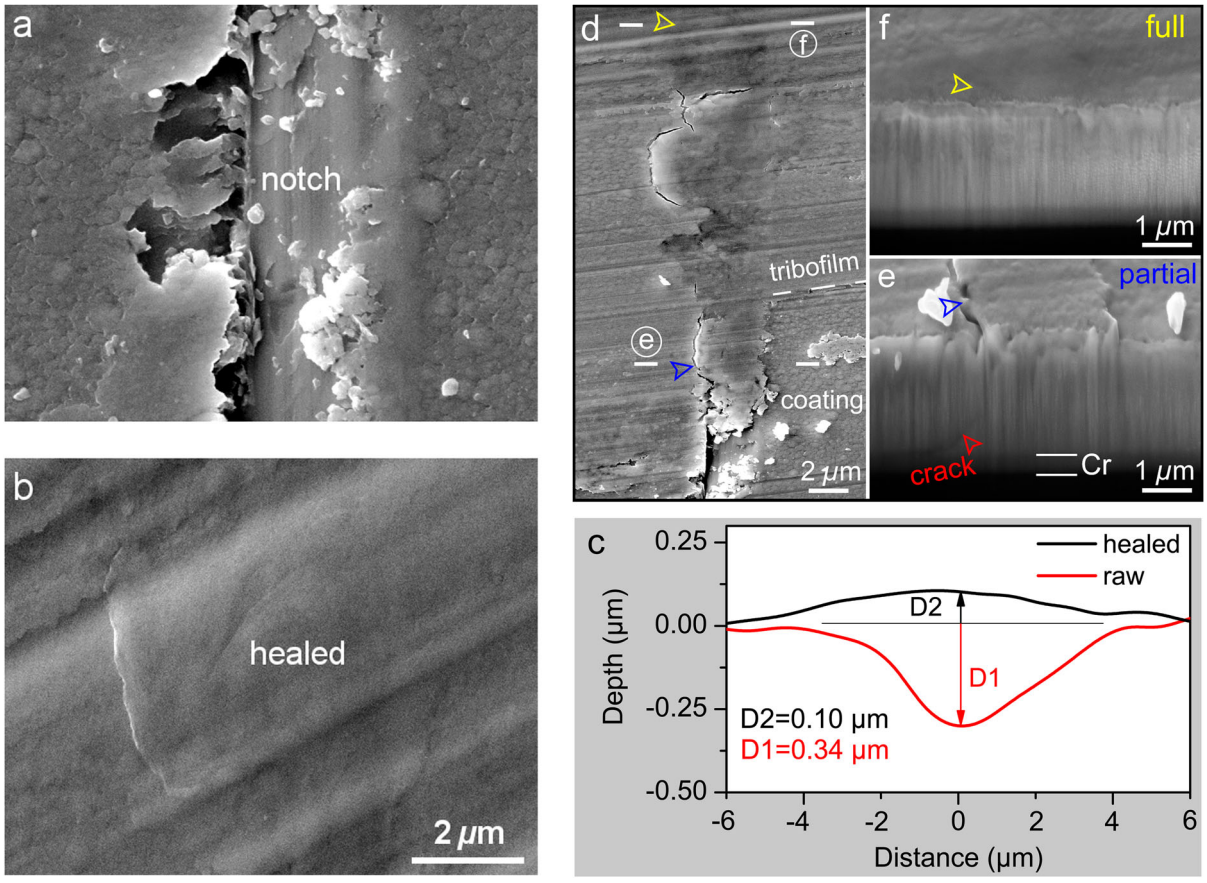

Figure 2. SEM images of a representative pre-notch (a) and after being healed (b) by the 'patching effect' of the tribofilm; (c) typical transverse profiles of the pre-notch before and after being healed; (d) SEM micrograph showing gradual crack self-healing behavior from the edge towards the center of the wear track and (e,f) FIB-cut cross-sections of the healed pre-notch with the locations marked in (d). Note that open arrows of the same colors indicate the identical locations.

platelets diverge into two directions with one parallel to the coating surface (i.e. ball sliding direction) and the other along the coating/notch interface. Figure 3(c–f) show that those platelets flexibly orientate themselves along the interface. Figure 3(g) indicates that WS_2 platelets start to converge out of the notch, in opposition to the branch shown in Figure 3(b). Noticeably, tens of nm thick layer of WS_2 (002) platelets, although partially damaged by Ga ion irradiation at the top, are observed perfectly aligned at the top part of the healed section (see Figure 3(h) and more details in Figure S4). The WS_2 platelets are much densified but randomized at the middle part of healed section (see Figure 3(i)).

The bottom part of the healed notch is magnified in Figure 4, which at nanometer scale reveals that WS_2 platelets tend to follow and spread over the whole curved interface, as indicated by the dashed line. No obvious defects such as voids or micro-cracks are found along the interface. This provides a solid evidence for the self-healing mechanism in the tribocoating.

It should be emphasized that the so-called TMD (002) basal plane subsurface reorientation were reported to be exclusively parallel with the coating surface [18–20], namely, the expected 'straight' TMD rearrangement parallel with the siding direction of the counterpart ball as seen in Figure S4(b). An intriguing finding in this study, however, is that WS_2 platelets can self-adapt themselves under sliding contact, forcing nano-laminae to dynamically favor the shearless (002) orientation where WS_2 basal planes are self-adjusting themselves conformally parallel to the curved interface. Thus, reorientation does not occur necessarily parallel with the top coating surface under sliding contact, but rather with local sliding along the interface of the healed notch during tribofilm filling and further densification. For instance, Figure 3(f) indicates the angle between a local reorientation of WS_2 platelets and ball sliding direction is around 40° rather than zero. The implication is that short WS_2 platelets can re-orientate and link to form continuous tribofilm for healing damage regardless of their shape although under cyclic contact sliding stimuli. In other words, such tribofilm can be deliberately driven or guided to form and flexibly fill up the very complex crack patterns.

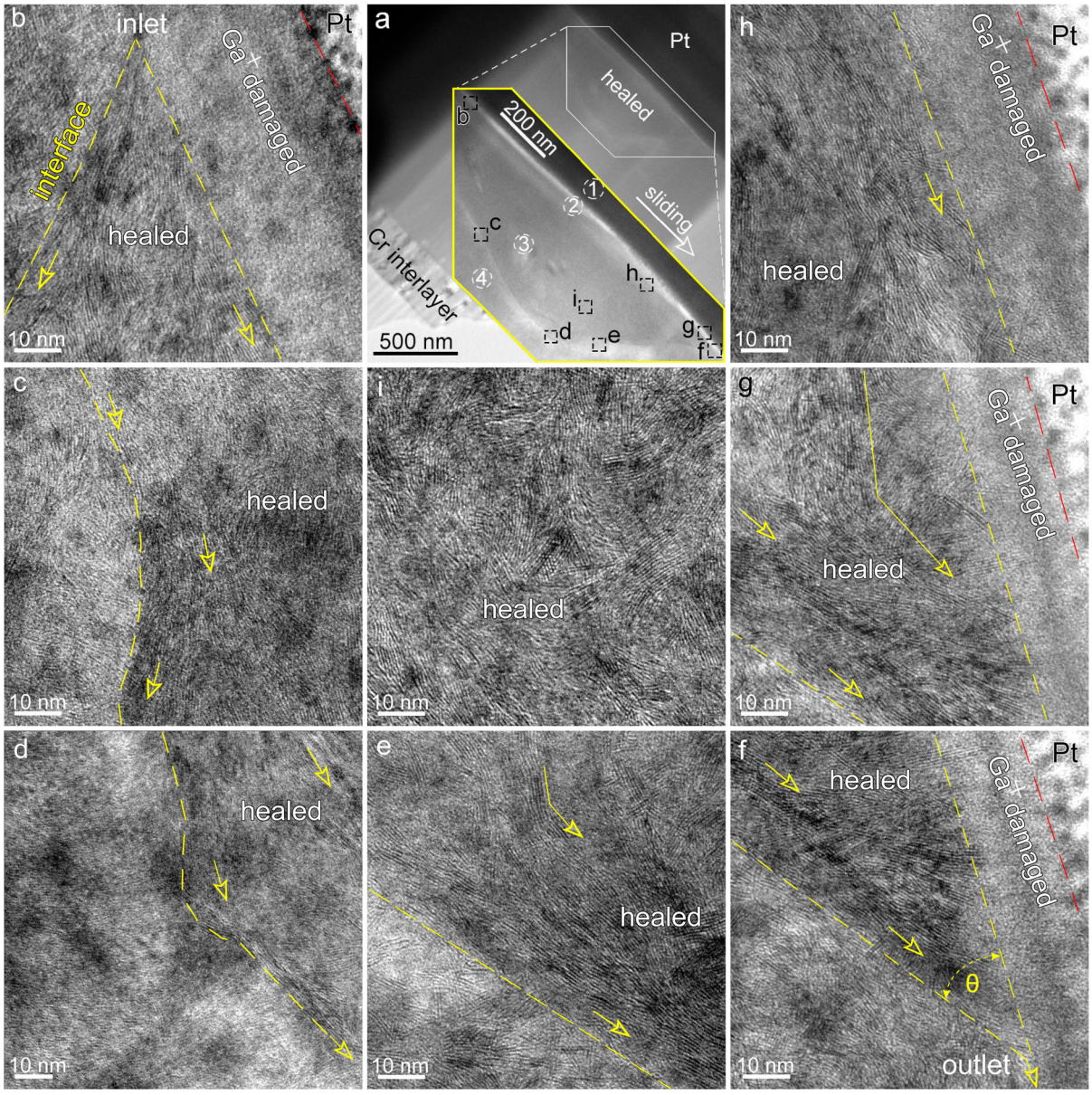

Figure 3. HR-TEM micrographs showing a panoramic cross-section of the healed notch: (a) overview of the self-healed notch with the marked box for higher magnification observation; (b–g) HR-TEM images showing WS_2 platelets re-orientated parallel to the local surface of the pre-notch; (h) HR-TEM image showing well aligned WS_2 platelets in the surface of the healed part parallel to the sliding direction; (i) HR-TEM image showing densified but randomly orientated WS_2 platelets in the center of the healed part.

Note that in the original coating WS_2 platelets are very short ($<$ 5 nm in length, see Figure S5) and randomly orientated in an amorphous carbon matrix. It is in strong contrast to Figure 4(b) where WS_2 platelets are apparently aligned and connected over the interface, suggesting the potential of such patches to heal irregular notches/cracks. WS_2 platelets are also elongated and densified near the interface, as illustrated by Figure 4(c), due to the crystallization of WS_2 even from an amorphous state under cyclic loading [21]. HR-TEM observations in Figure S6 show that the oxidation of WS_2 into WO_3 may locally block or diverge the perfect alignment of WS_2 basal plane.

Figure 5 shows the schematics of the self-healing process where tribofilms heal a pre-notch damage. Note that the damage healing behavior is a more or less autonomous process where the damage itself initiates the healing process under the sliding stimuli. More importantly, the healing agent directly originates from the bulk coating. In fact, the notched damages are acting as microreservoir and provide WS_2 lubricants continuously. Therefore, damage at the surface may be healed with beneficial effects in lubrication, as restored by the entangled layered WS_2 patches in the tribofilm. Such intrinsic mechanism is potentially superior to the extrinsic

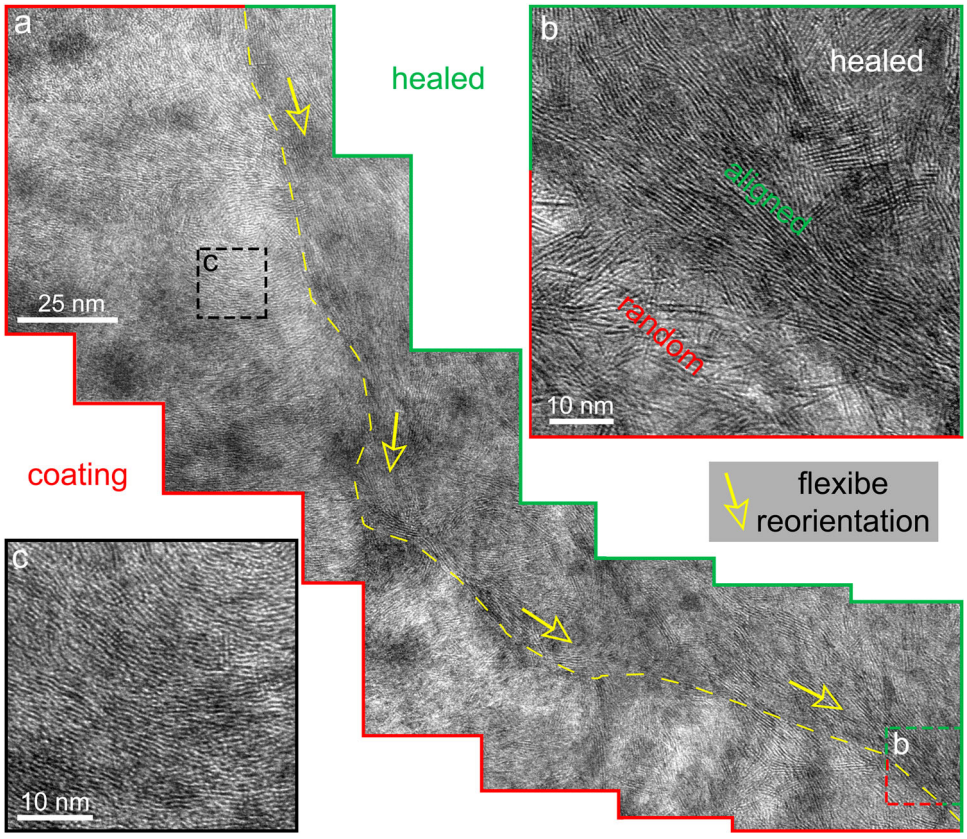

Figure 4. (a) Stitched HR-TEM micrographs revealing reorientated WS_2 platelets along the curving interface at the bottom of the notch; (b) HR-TEM image (higher magnification of Figure 3(e)) distinguishing well aligned WS_2 (002) platelets in the healed notch from short and random ones in the raw coating; (c) HR-TEM image of the enriched and elongated WS_2 platelets near the interface. The dashed line indicates the tortuous interface of the healed notch/coating.

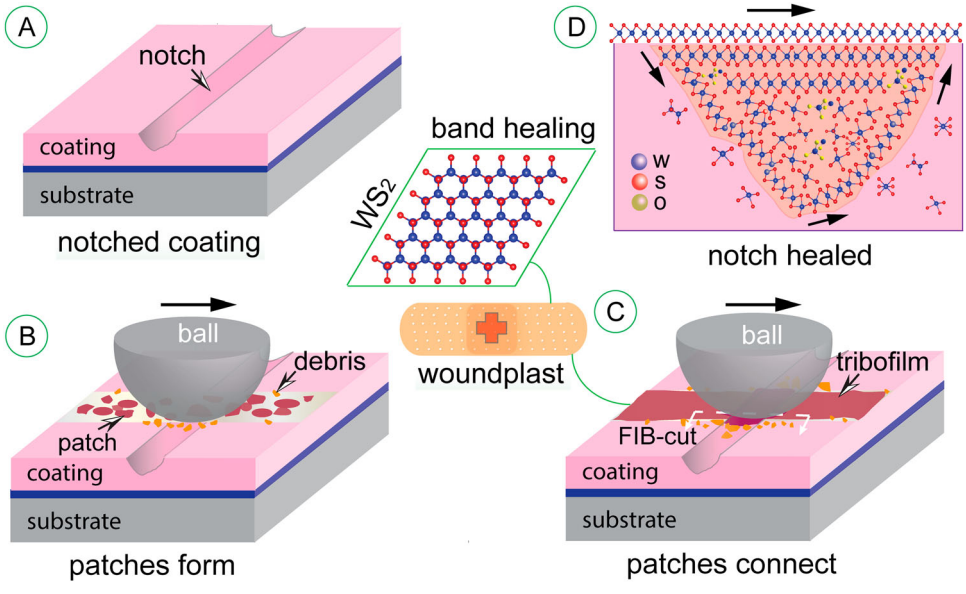

Figure 5. Schematic illustration of the self-healing process where tribofilms reverse damages to work: (a) a pre-notch made in WS_2/a-C coating; (b) patchy tribofilms start to form; (c) tribofilms interconnect and fill into the notch; (d) cross-section image sliced at the healed part by FIB showing that WS_2 (002) platelets adapt themselves to flexibly overspread the curved coating/notch interface, whereas at the top of the healed notch such platelets are well re-orientated parallel to the sliding direction exhibiting ultra-low friction.

approaches (which are restricted due to the exhaust of the healing agents) as reported in previous studies, e.g. externally pre-store TMD powders or coatings into the textured reservoirs of less lubricating materials as to enhance their tribological performance [17,22–24] or exploit the conformity of atomic layer deposition (ALD) of external top layers to seal pinholes of columnar-like coatings [25].

4. Conclusions

In summary, this study elucidates potential self-healing mechanisms in tribocoatings, as illustrated by the nanocomposite WS_2/a-C coatings where the in-situ formed flexible tribofilms autonomously 'patch' voids and heal cracks under sliding contact during real tribological service, thereby prolonging the lifetime of the coated substrate in an economic and sustaining way. This sheds light on potential release of the requirement of producing flawless coatings for triboapplications in industry.

Acknowledgments

Professor Wesley Browne of the University of Groningen, the Netherlands is gratefully acknowledged for his support with Raman spectroscopy.

Disclosure statement

No potential conflict of interest was reported by the authors.

Funding

This work was supported by China Scholarship Council [CSC, grant number 201406160102].

ORCID

Yutao Pei http://orcid.org/0000-0002-1817-2228

References

[1] Hager MD, Greil P, Leyens C, et al. Self-healing materials. Adv Mater. 2010;22:5424–5430.
[2] Blaiszik BJ, Kramer SLB, Olugebefola SC, et al. Self-healing polymers and composites. Annu Rev Mater Res. 2010;40:179–211.
[3] White SR, Sottos NR, Geubelle PH, et al. Autonomic healing of polymer composites. Nature. 2001;409(6822):794–797.
[4] Kirkby EL, Rule JD, Michaud VJ, et al. Embedded shape-memory alloy wires for improved performance of self-healing polymers. Adv Funct Mater. 2008;18(15):2253–2260.
[5] Joshi S, Goyal S, Mukherjee A, et al. Microbial healing of cracks in concrete: a review. J Ind Microbiol Biotechnol. 2017;44(11):1511–1525.
[6] Jonkers HM, Thijssen A, Muyzer G, et al. Application of bacteria as self-healing agent for the development of sustainable concrete. Ecol Eng. 2010;36(2):230–235.
[7] Yang HJ, Pei YT, Rao JC, et al. High temperature healing of Ti_2AlC: on the origin of inhomogeneous oxide scale. Scr Mater. 2011;65(2):135–138.
[8] Yang HJ, Pei YT, Rao JC, et al. Self-healing performance of Ti_2AlC ceramic. J Mater Chem. 2012;22(17):8304–8313.
[9] Banerjee T, Chattopadhyay AK. Structural, mechanical and tribological properties of WS_2-Ti composite coating with and without hard under layer of TiN. Surf Coat Technol. 2014;258:849–860.
[10] Cao HT, Wen F, Kumar S, et al. On the S/W stoichiometry and triboperformance of $WS_xC(H)$ coatings deposited by magnetron sputtering. Surf Coat Technol. 2018 (in press). doi:10.1016/j.surfcoat.2018.04.040.
[11] Lévy F, Moser J. High-resolution cross-sectional studies and properties of molybdenite coatings. Surf Coat Technol. 1994;68-69:433–438.
[12] Pei YT, Galvan D, De Hosson JTM. Nanostructure and properties of TiC/a-C:H composite coatings. Acta Mater. 2005;53:4505–4521.
[13] Polcar T, Evaristo M, Cavaleiro A. Self-lubricating W-S-C nanocomposite coatings. Plasma Process Polym. 2009;6(6-7):417–424.
[14] Ren S, Li H, Cui M, et al. Functional regulation of Pb-Ti/MoS_2 composite coatings for environmentally adaptive solid lubrication. Appl Surf Sci. 2017;401:362–372.
[15] Muratore C, Voevodin AA. Chameleon coatings: adaptive surfaces to reduce friction and wear in extreme environments. Annu Rev Mater Res. 2009;39:297–324.
[16] Cao HT, De Hosson JTM, Pei YT. Effect of carbon concentration and argon flow rate on the microstructure and triboperformance of magnetron sputtered WS_2/a-C coatings. Surf Coat Technol. 2017;332:142–152.
[17] Wang DS, Hu M, Jiang D, et al. Preparation and characterization of the CrN nanocone array textured WS_2 film. Mater Lett. 2017;188:267–270.
[18] Cao HT, Wen F, De Hosson JTM, et al. Instant WS_2 platelets reorientation of self-adaptive WS_2/a-C tribocoating. Mater Lett. 2018;229:64–67.
[19] Moser J, Lèvy F. MoS_{2-x} lubricating films: structure and wear mechanisms investigated by cross-sectional transmission electron microscopy. Thin Solid Films. 1993;228:257–260.
[20] Sundberg J, Nyberg H, Särhammar E, et al. Influence of Ti addition on the structure and properties of low-friction W-S-C coatings. Surf Coat Technol. 2013;232:340–348.
[21] Xu J, He TF, Chai LQ, et al. Selective-releasing-affected lubricant mechanism of a self-assembled MoS_2/Mo–S–C nanoperiod multilayer film sliding in diverse atmospheres. Phys Chem Chem Phys. 2017;19(12):8161–8173.
[22] Voevodin AA, Zabinski JS. Laser surface texturing for adaptive solid lubrication. Wear. 2006;261(11-12):1285–1292.
[23] Wu Z, Xing YQ, Huang P, et al. Tribological properties of dimple-textured titanium alloys under dry sliding contact. Surf Coat Technol. 2017;309:21–28.
[24] Lian YS, Chen HF, Deng JX, et al. Preparation and property characterization of WS_2 coatings deposited on micro-nano textured surfaces of cemented carbide at different WS_2 target currents. Int J Refract Metals Hard Mater. 2018;72:286–291.
[25] Härkönen E, Kolev I, Díaz B, et al. Sealing of hard CrN and DLC coatings with atomic layer deposition. ACS Appl Mater Interface. 2014;6(3):1893–1901.